ELSEVIER

Catalysis Today 65 (2001) 335–341

CATALYSIS TODAY

www.elsevier.com/locate/cattod

Hydrogenation active sites of unsupported molybdenum sulfide catalysts for hydroprocessing heavy oils

Y. Iwata [a], Y. Araki [a], K. Honna [a], Y. Miki [b], K. Sato [b], H. Shimada [b,*]

[a] *Tsukuba-branch, Advanced Catalyst Research Laboratory, Petroleum Energy Center, 1-1 Higashi, Tsukuba, Ibaraki 305-8565, Japan*
[b] *National Institute of Materials and Chemical Research, 1-1 Higashi, Tsukuba, Ibaraki 305-8565, Japan*

Abstract

The purpose of the present study was to elucidate the nature of the hydrogenation active sites on unsupported molybdenum sulfide catalysts, aimed at the improvement of the catalysts for the slurry processes. The number of hydrogenation active sites was found to relate to the "inflection" on the basal plane of the catalyst particles. The comparison of the catalytic activity to that of an oil-soluble catalyst in the hydroprocessing of heavy oils suggests that the performance of the oil-soluble catalyst was near the maximum, unless another component such as Ni or Co was incorporated.

Keywords: Dispersed catalyst; Ammonium tetrathiomolybdate; NO chemisorption; X-ray diffraction; Molybdenum dithiocarbamate

1. Introduction

For hydroprocessing heavy oils with residues, slurry processes with dispersed catalysts have many advantages over conventional fixed-bed processes [1,2]. Some past studies [2,3] pointed out that unsupported molybdenum sulfide (MoS_2) is a promising candidate of the ultra fine particle catalyst in the slurry processes [2,3]. The primary function required for the catalysts in the slurry processes is not hydrodesulfurization (HDS) but hydrogenation (HYD), because the major role of the catalyst is to quench thermally produced radicals by supplying active hydrogen species. The present study has been conducted for better understanding on the HYD active sites of unsupported MoS_2 catalysts, aimed at the improvement of catalysts in the slurry processes.

In a previous study [4], the present authors compared three kinds of unsupported MoS_2 catalysts with similar surface area but with different morphologies. The results indicated that the HYD active sites were formed on a highly bent multi-layered MoS_2 structure. This suggested that the curvature of the basal planes was active for HYD. The purpose of the present paper is to further investigate the genesis of the HYD active sites on the basal plane of the MoS_2 structure. For this purpose, the authors have prepared several kinds of powdered catalysts starting from ammonium tetrathiomolybdate and compared the catalytic activities and properties. In addition, the performance of the unsupported catalyst in the hydroprocessing of heavy oils was compared with that of an oil-soluble catalyst to estimate the maximum activity of MoS_2 based catalysts that might be available.

2. Experimental

2.1. Sample preparation

The catalysts were obtained by thermal decomposition of ammonium tetrathiomolybdate ($(NH_4)_2MoS_4$,

* Corresponding author. Fax: +81-298-61-4534.
E-mail address: shimada@nimc.go.jp (H. Shimada).

0920-5861/01/$ – see front matter
PII: S0920-5861(00)00554-X

ATTM) in a stream of 10% H_2S/H_2 gas mixture. The decomposition temperature was varied from 623 (350°C) to 973 K (700°C). After reaching the decomposition temperature with a heating rate of 2 K/min, the temperature was kept for 1 h. The catalysts were named as TD350∼TD700 depending on the decomposition temperature.

2.2. Activity measurement

The HYD activities of the catalysts were determined using a 25 wt.% 1-methylnaphthalene (1-MN)/tetradecane solution as a model reactant. The reactions were carried out at 603 K for 1 h in a batch reactor (35 cm^3). The initial charge to the reactor was 10 cm^3 of the reactant and 6.0 MPa of H_2. The amount of the catalyst was changed from 0.05 to 0.20 g to perform kinetic analysis. The product analysis procedures were described in a previous report [4].

Hydroprocessing of Arabian heavy atmospheric residue (AH-AR) containing 45.6% of vacuum residue (b.p. > 793 K, VR) with 6.6% of asphaltene and 4.22% of sulfur was carried out at 683 K in an autoclave (136 cm^3). The initial charge was 10 g of AH-AR and 10 MPa of H_2. The catalysts used were the above described TD350 and molybdenum dithiocarbamate ($([(C_8H_{17})_2NC])_2S_6Mo_2O_2$, MoDTC) as an oil-soluble catalyst. The catalytic activities were compared in terms of asphaltene removal, VR conversion and HDS.

2.3. Catalyst characterization

The BET surface areas were measured after degassing the sample in vacuum at 423 K. The transmission electron microscopic (TEM) observation was conducted with an accelerated voltage of 200 kV. The X-ray diffraction (XRD) patterns were recorded using Cu Kα X-rays (0.154 nm) with a scan speed of 0.02°.

The chemical NO uptake was determined with a volumetric adsorption method using an automatic instrument (Micromeritics ASAP 2010C). Prior to the NO adsorption, each catalyst was treated in a stream of He or H_2 at a temperature ranging from 423 to 723 K for 1 h. The catalyst was subsequently evacuated down to 1×10^{-3} Pa and then cooled down to 308 K. The amount of NO adsorbed was measured at 308 K over the pressure range of 1∼60 kPa. After measuring the first isotherm, the catalyst was evacuated at 308 K for 2 h and then the second isotherm was measured. The chemical adsorption isotherm was obtained, taking the difference between the first and second isotherm profiles, because the first isotherm was a measure of the combined chemical and physical adsorption, the second isotherm being that of the physical adsorption.

3. Results

3.1. Catalytic activities

To quantitatively compare the HYD activities of the catalysts, the reaction rate constants were calculated by assuming a pseudo-first order reaction mechanism, $d[1\text{-MN}]/dt = -k[1\text{-MN}]$. The assumption was consistent with the reaction data up to the conversion of 50% as previously shown [4]. Table 1 summarizes the reaction rate constants $k_{(1\text{-MN})}$ obtained by the above procedures and the relative rate constants k_r relative to that over TD350. k_r decreased with rising decomposition temperature.

Table 2 shows the comparison of the catalytic activities of TD350 and MoDTC in the hydroprocessing of AH-AR. In terms of VR conversion and HDS, the catalytic activity of 100 mg of TD350 was almost comparable to that of 10 mg of MoDTC. Evidently, the asphaltene conversion over TD350 was lower than that over 10 mg of MoDTC. As described in the

Table 1
Rate constants for HYD of 1-MN over the catalysts

	TD350	TD400	TD450	TD500	TD550	TD600	TD700
$k_{(1\text{-MN})}$ [a]	788	775	745	516	246	99.0	64.8
k_r [b]	1.00	0.97	0.93	0.65	0.31	0.12	0.081

[a] Rate constants in 10^{-7} mol/(mol of Mo) s.
[b] Relative rate constants, relative to that of TD350.

Table 2
Hydroprocessing of AH-AR over TD350 and MoDTC

	Reaction time (h)	TD350 (100 mg[a])	MoDTC	
			50 mg	10 mg
HDAs[b] (%)	6		88	57
	9	51	92	
	12		97	79
VR conversion (%)	6		46	39
	9	47	53	
	12		60	52
HDS[c] (%)	6		77	40
	9	52	83	
	12		89	70

[a] Catalyst weight as Mo metal.
[b] Asphaltene (hexane insoluble) removal.
[c] Sulfur removal.

introduction, the most important role of the catalyst in the primary upgrading is to quench thermally produced radicals and to prevent retrogressive reactions. In fact, hydroprocessing AH-AR under the same conditions without catalyst increased the asphaltene content by 15–20%. This implies that the activity of MoDTC in hydroprocessing AH-AR is more than one magnitude higher than that of TD350.

3.2. Catalytic properties

Table 3 shows the summary of the catalyst characterization. All the catalysts exhibited relatively low BET surface area values of 5–10 m^2/g. In particular, high temperature decomposition over 773 K (500°C) significantly decreased the surface area. The bulk chemical analysis indicated that all the catalysts were with almost stoichiometric MoS_2 compositions.

Fig. 1 shows the TEM photographs of TD350, TD550 and TD700. The fringes observed in the photographs had a spacing of about 0.6 nm that was characteristic of the (0 0 2) basal planes of crystalline MoS_2. Each crystalline MoS_2 consisted of several slabs with lengths over 10 nm. The image of TD350 clearly displays that MoS_2 slabs are highly bent and folded. The curvature of the layers decreased with rising decomposition temperature and some of the slabs observed in TD700 were almost straight.

Fig. 2 shows the XRD patterns of the catalysts in comparison with that of commercially available MoS_2 powders. The patterns of the catalysts were characteristic of poorly crystallized MoS_2 structures as indicated by the broad peaks. The crystallite dimensions parallel, La, and normal, Lc, to the basal plane can be estimated using the Scherrer's equation [5]. After deconvoluting the profiles, La and Lc were calculated respectively using the linewidths of the (1 0 0) and (0 0 2) reflection peaks (Table 3). Table 3 indicates that the MoS_2 crystallites grows both in parallel and normal directions to the basal plane with rising decomposition temperature.

Fig. 3 shows the NO adsorption isotherms for TD450 reduced at 573 K in a stream of hydrogen. The chemical uptake exhibited a gradual increase with pressure. This is presumably due to the fluctuation of the NO adsorption from the ideal Langmuir-type adsorption in which the amount of chemisorption reaches a constant at a high pressure region. We

Table 3
Summary of the characterization of MoS_2 catalysts

Catalyst	SA (m^2/g)[a]	S/Mo (–)	La (nm)[b]	Lc (nm)[c]	SA (m^2/g)[d]	NO/Mo (%)
TD350	9	2.1	4.5	2.6	345	5.0
TD400	9	2.0	5.2	3.0	299	4.6
TD450	10	2.1	5.6	3.2	279	4.0
TD500	8	2.1	6.3	3.8	242	3.7
TD550	7	2.2	8.3	4.7	189	2.4
TD600	6	2.0	8.9	5.8	166	1.3
TD700	5	2.0	10.7	10.5	118	0.2

[a] Surface area obtained by BET method.
[b] Crystallite dimension parallel to the basal plane.
[c] Crystallite dimension normal to the basal plane.
[d] Surface area calculated from La and Lc.

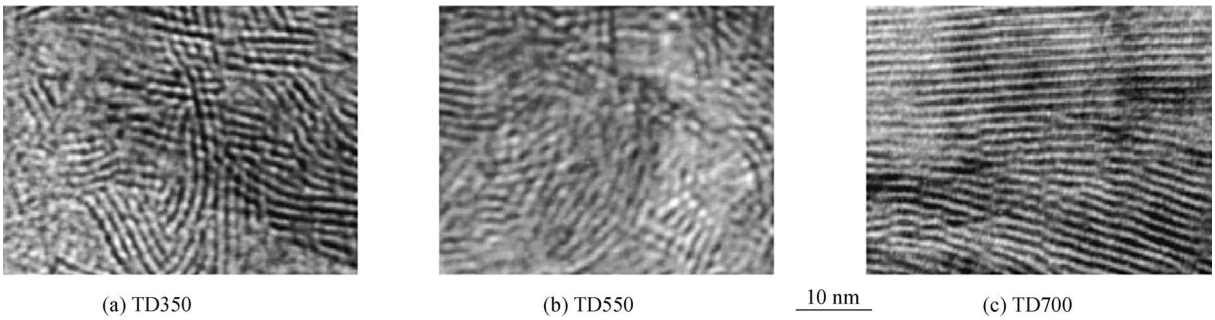

Fig. 1. TEM photographs of the catalysts.

defined the chemical NO uptake by extrapolating the profile in the region between 10 and 60 kPa to zero pressure as inserted in Fig. 3.

Fig. 4 shows the effect of the pretreatment on the chemical NO uptake on TD450. The pretreatment by hydrogen significantly increased the NO uptake. When the catalyst was treated under a flow of He or reduced at 423 K, the number of sulfur vacancies was small. In contrast, the high temperature reduction at 723 K, presumably resulted in the aggregation or destruction of the MoS_2 structure. Considering the reaction conditions (603 K, 6.0 MPa), we determined the NO uptake after the hydrogen pretreatment at 573 K. Fig. 5 shows the relationship between the NO/Mo in Table 3 and the HYD rate constant in Table 1. A good relationship implies that the number of NO chemisorption sites is proportional to the number of HYD active sites. If NO was chemisorbed on the edge planes of MoS_2 [6], the HYD active sites almost coincide with the edge sites.

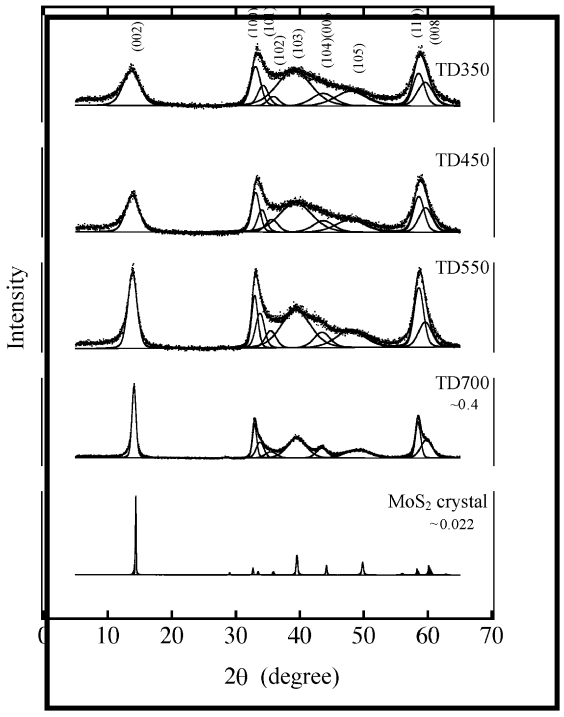

Fig. 2. XRD patterns of the catalysts and MoS_2 crystal with curve fitting analysis.

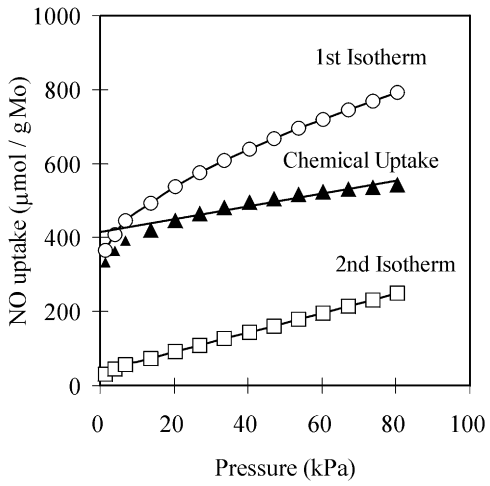

Fig. 3. NO adsorption isotherms for TD450 reduced at 300°C in a flow of H_2. Circle: 1st isotherm, square: 2nd isotherm, triangle: difference (chemical uptake).

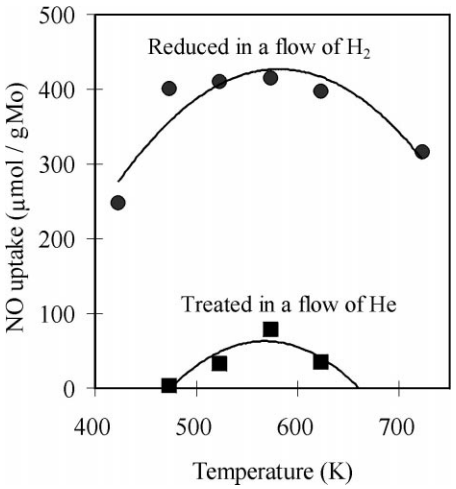

Fig. 4. Effect of pretreatment on NO chemical uptake for TD450.

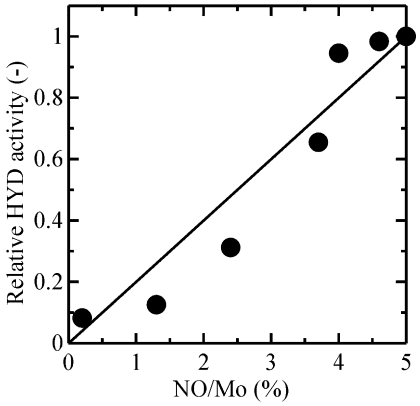

Fig. 5. Relationship between the HYD activity and NO uptake on the catalysts.

4. Discussions

4.1. Structural model

Before the discussion on the HYD active sites, we will propose a structural model using the characterization results in Table 3. If one assumes that each catalyst particle consists of a hexagonal MoS_2 crystallite with the dimensions given by XRD, the surface area of the catalyst can be calculated using the following equation,

$$SA^* = 1000\frac{(2La + 4Lc)}{La\,Lc\,d}\ (m^2/g)$$

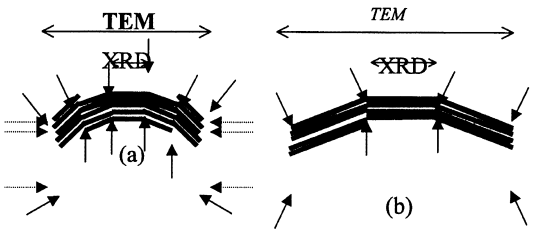

Fig. 6. Schematic drawing of the catalyst structures: (a) catalyst decomposed at lower temperatures and (b) catalyst decomposed at higher temperatures. Solid arrows: HYD active sites; dotted arrows: edge sites except rim sites.

where La and Lc are the crystallite dimensions in nanometers and d is 4.8 in cubic centimeters per gram. Table 3 shows the calculated surface area values, SA^*, that are significantly larger than the corresponding BET surface area values, SA. For instance, SA^* of TD350 is calculated at 345 m^2/g, while the BET surface area is 9 m^2/g. This discrepancy can be solved by the TEM photograph (Fig. 2), in which the lengths of the MoS_2 slabs are much larger than La, but with much curvature. Namely, XRD measures the lateral dimensions of microdomains that are a part of each MoS_2 particle. Fig. 6 shows schematic drawing of the catalyst particle deduced from the above discussions. With rising the decomposition temperature, the lateral dimensions of microdomains increase together with the increase in the particle size.

Some previous papers [7–9] reported much higher surface area values of unsupported MoS_2 catalysts prepared by decomposition of ammonium tetrathiomolybdate. The discrepancy between the present and those studies is likely due to different heating rates in the catalyst preparation. Naumann et al. [7] reported that the surface area of MoS_2 could be controlled from 5 to 158 m^2/g by changing the heating rates. We also prepared a MoS_2 catalyst with a surface area value of 61 m^2/g by the heating rate of 50 K/min; however, the catalytic activity of the high surface area catalyst was comparable to that of TD350 [10]. This is probably due to the aggregation of the microdomains at the early stage of the reaction, because the high surface area of the "rapid decomposition catalyst" was significantly decreased after the reaction [10]. Therefore, we prefer the aggregated particle model in Fig. 6 to the isolated microdomain models that is solely based on the XRD dimensions.

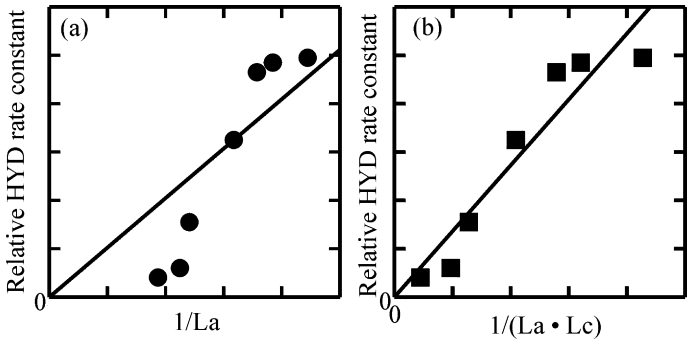

Fig. 7. Relationship between the crystallite dimension and the relative HYD rate constant: (a) 1/La vs. HYD rate constant, (b) 1/(La Lc) vs. HYD rate constant.

4.2. HYD active sites

In spite of the model proposed in Fig. 6, we first assume that all the microdomains are isolated and exposing their external surface in the following discussion. Many past studies [11,12] have pointed out that all the catalytic activities are closely associated with the edge planes of MoS_2 crystal where sulfur vacancies are more easily formed than the basal planes. In this case, the number of catalytic active sites would be inversely proportional to the lateral dimension, La. As shown in Fig. 7(a), however, this is not the case. According to the "rim-edge model [13]" in which only the rim layers (top and bottom layers of the slabs) provide active sites for HYD of aromatic rings, the number of active sites would be proportional to 1/(La Lc). The relationship in Fig. 7(b) is evidently much better than that in Fig. 7(a). This suggests that the edge planes of the microdomains except the rim layers are not active for HYD, or at least much less active for HYD than the rim layers.

Now, let us return to the structural model in Fig. 6. When the microdomains aggregate and form a large particle, most of the edge planes are not any more exposed as shown in Fig. 6(a). In contrast, the rim sites of the microdomains are exposed as the "inflection" indicated by solid arrows in Fig. 6. The active sites on the "inflection" are dominant as compared with that on the edge sites of the MoS_2 particle indicated by the dotted arrows. This would make an approximately linear relationship between the HYD rate constants and 1/(La Lc) in Fig. 7(b).

Thus, the present results are seemingly consistent with the "rim-edge model [13]". In the "rim-edge model", HYD cannot be catalyzed on the edge plane except the rim layers, because aromatic rings cannot be adsorbed with the η^6 coordination due to steric hindrance. Our discussion does not preclude the HYD active sites on the edge plane of the MoS_2 particle (indicated by dotted arrows in Fig. 6). Rather, Fig. 5 indicates that the HYD reactions are catalyzed on all the NO adsorption sites that are likely located on all the edge sites [6]. The relationship between the HYD and HDS active sites will be discussed elsewhere.

From the macro point of view, for instance by the TEM observation, the basal plane of the MoS_2 particle provides catalytically active sites when the MoS_2 layers are with curvatures. This indicates that the number of HYD active sites increases with decreasing number of slabs in each MoS_2 particle. This is in very good agreement with the previous discussion on the supported MoS_2 catalysts [14] that the catalysts with single layer slabs are more active than those with multi-layer slabs.

4.3. Maximum activities for AR-AH

Fig. 5 shows that the NO uptake per Mo atom for TD350 is about 5%. As discussed in Section 3.1, the activity of MoDTC was more than one magnitude higher than that of TD350. These suggest that the maximum activity of MoS_2 based catalyst could not be improved over two times that of MoDTC, even when the MoS_2 can be completely dispersed. To overcome this limitation, the enhancement of intrinsic activity, for instance, the incorporation of another component such as Co or Ni is needed.

It is essential to minimize the catalyst particle size to maximize the catalytic activity. In addition, the discussions in the previous section indicates the importance of microdomain sizes of MoS_2 crystallites that would result in much "inflection" on the basal plane of the catalyst particles. Further, the prevention of aggregation and growth of MoS_2 microdomains is important to minimize the catalyst deactivation during the reaction. The incorporation of another component may also be useful from this point of view.

5. Conclusion

In the present study, the HYD active sites of MoS_2 particles have been investigated to obtain a clue for the improvement of dispersed MoS_2 catalysts in the primary upgrading of heavy oils. The results showed that the HYD active sites of MoS_2 particles were associated with the "inflection" on the basal plane that correspond to the "rim" sites of crystalline MoS_2 microdomains. This explains the reason why the MoS_2 catalysts with curved slabs are active for HYD of aromatic rings. To increase the number of "inflection", the growth of the microdomains should be suppressed. It is recommended to incorporate other components, such as Ni or Co, that would not only enhance the catalytic activities but also prevent the growth and aggregation of the microdomains.

Acknowledgements

This work was carried out as a research project of the Petroleum Energy Centre and was supported by the Ministry of International Trade and Industry.

References

[1] F. Morel, S. Kressmann, V. Harlé, S. Kasztelan, Stud. Surf. Sci. Catal. 106 (1997) 1.
[2] A. Del Bianco, N. Panarti, S. Di Carlo, J. Elmouchnino, B. Fixari, P. Le Perchec, Appl. Catal. A 94 (1993) 1.
[3] S. Peureux, S. Bonnamy, B. Fixari, F. Lambert, P. Le Perchec, B. Pepin-Donat, M. Vrinat, B. Soc. Chim. Belg. 104 (1995) 359.
[4] Y. Iwata, K. Sato, T. Yoneda, Y. Miki, Y. Sugimoto, A. Nishijima, H. Shimada, Catal. Today 45 (1998) 353.
[5] P. Scherrer, Göttingen Nachr., 2 (1918) 98.
[6] N.Y. Topsøe, H. Topsøe, J. Catal. 84 (1983) 386.
[7] A.W. Naumann, A.S. Behn, E.M. Thorsteinson, Proceedings of Fourth International Conference on Chemistry and Uses of Molybdenum, Climax Molybdenum Co., 1982, p. 313.
[8] C. Calais, N. Matsubayashi, C. Geantet, Y. Yoshimura, H. Shimada, A. Nishijima, M. Lacroix, M. Breysse, J. Catal. 174 (1998) 130.
[9] D.G. Kalthod, S.W. Weller, J. Catal. 95 (1985) 455.
[10] Y. Araki, Y. Iwata, Y. Miki, K. Honna, N. Matsubayashi, H. Shimada, Stud. Surf. Sci. Catal. 127 (1999) 69.
[11] R.R. Chianelli, Catal. Rev. Sci. Eng. 26 (1984) 361.
[12] S. Kasztelan, L. Jalowiecki, A. Wambeke, J. Grimblot, J.P. Bonnelle, B. Soc. Chim. Belg. 96 (1987) 1003.
[13] M. Daage, R.R. Chianelli, J. Catal. 149 (1994) 414.
[14] M. Vrinat, M. Breysse, C. Geantet, J. Ramirez, F. Massoth, Catal. Lett. 26 (1994) 25.